Three coupled ultraslow temporal solitons in a five-level tripod atomic system

Wen-Xing Yang,[1,2,*] Ai-Xi Chen,[3] Liu-Gang Si,[4] Kaijun Jiang,[5] Xiaoxue Yang,[4] and Ray-Kuang Lee[2]

[1]*Department of Physics, Southeast University, Nanjing 210096, People's Republic of China*

[2]*Institute of Photonics Technologies, National Tsing-Hua University, Hsinchu 300, Taiwan*

[3]*Department of Applied Physics, School of Basic Science, East China Jiaotong University, Nanchang 330013, People's Republic of China*

[4]*School of Physics, Huazhong University of Science and Technology, Wuhan 430074, People's Republic of China*

[5]*Laboratoire Kastler-Brossel, École Normale Supérieure (ENS), 24 rue Lhomond, 75005 Paris, France*

(Received 14 December 2008; revised manuscript received 9 July 2009; published 16 February 2010)

We propose a scheme to generate three coupled ultraslow optical solitons in a five-level tripod atomic system. We show that the detrimental distortions of the three weak probe fields due to dispersion effects under weak driving conditions can be well balanced by self- and cross-phase-modulation effects, which leads to the three coupled ultraslow temporal optical solitons with the temporal, group velocity, and amplitude values nearly matched. In contrast to other schemes, our model uses optical fibers, including multichromatic optical solitons in the stimulated Raman scattering, and produces three coupled ultraslow optical solitons in a small propagation distance of less than 1 cm with $\frac{1}{2}$ Rabi frequency of the driving field, typically less than 100 MHz.

DOI: 10.1103/PhysRevA.81.023814 PACS number(s): 42.65.Tg, 42.50.Gy, 05.45.Yv

I. INTRODUCTION

Optical solitons have been the subject of intense study because of their potential applications in optical communication systems and also in the development of optical switching devices. Optical solitons initially were described by a single nonlinear Schrödinger equation (NLSE) for a scalar field. Such scalar optical solitons form when a single light propagates inside a nonlinear medium in such a way that its polarization state is maintained. When these conditions are not satisfied, one must consider interaction of several field components at different frequencies or polarizations and solve simultaneously a set of coupled NLSEs. A shape-preserving solution of such equations is called a vector soliton because of its multicomponent nature. In recent years, considerable attention has been paid to the temporal [1–8] and spatial vector optical solitons [9–13] in various nonlinear systems. Because of their remarkable properties, vector optical solitons have promising applications for the design of new types of all-optical switches and logic gates [14].

However, most previous multicomponent optical solitons including temporal and spatial solitons were generated in passive optical media, such as optical fibers [4–15]. In this case, intense electromagnetic fields and long propagation distances are required, and far-off resonance excitation schemes are generally employed to avoid unmanageable attenuation and distortion. As a consequence, multicomponent optical solitons produced in this way generally travel with a propagation speed very close to velocity of light in vacuum. This makes the active control of solitons difficult because of the lack of distinctive energy levels and related transition selection rules. In particular, it is hard to realize Manakov [16] temporal optical solitons in optical fibers because the ratio between self-phase-modulation (SPM) and cross-phase-modulation (CPM) is not unity, and there is also detrimental energy exchange between each component due to the existence of the four-wave mixing effect. Manakov optical solitons are of great interest, not only because the described coupled NLSEs have interesting mathematical properties but also because such solitons may have promising practical applications (e.g., for realizing all-optical computing) [17]. In contrast to spatial Manakov optical solitons, which were observed more than 10 years ago [11], until now temporal Manakov vector optical solitons have not been realized in experiments.

It should be noted that electromagnetically induced transparency (EIT) [18] in cold atomic media has been vigorously pursued in the fields of nonlinear and quantum optics. It has been demonstrated that these techniques possess striking features and lead to interesting physical effects [19–27]. One is the significant reduction of group velocity [28,29], which may have technical applications [30]. Another feature is that Kerr nonlinearity of optical media can be largely enhanced through a CPM effect. This technique has been proposed for achieving a large nonlinear phase shift [19,21,27] and some other nonlinear optical processes under weak driving conditions. Based on large nonlinearity enhancement, low absorption, and ultraslow propagation properties, it has been shown recently that it is possible to produce a new type of optical soliton, an ultraslow optical soliton (USOS), in cold atomic media [31–36] as well as in semiconductor solid-state devices [37–39]. Because of their robust nature with a ultraslow propagating velocity, USOSs have the potential for well-characterized, distortion-free optical pulses and hence have technological applications in optical and telecommunication engineering.

In this work, we show the propagation of shape-preserved optical pulses in the form of three coupled temporal components, in which group velocity and amplitude are possible to match in a five-level tripod atomic system. In the presence of a continuous wave (cw) coherent classical control field, the absorption of the three probe fields can be almost suppressed while simultaneously the nonlinearity is enhanced under appropriately conditions. By employing the density-operator formalism to describe the interaction of the system, we demonstrate that the SPM and CPM effects can balance the dispersion and result in three coupled nonlinear Schrödinger equations for the propagation of three weak probe fields, which admit solutions for three coupled optical solitons. Compared

*wenxingyang2@126.com

with the passive schemes (such as optical fibers [4–15]) as well as multichromatic solitons induced by stimulated Raman scatterings [40,41], the solitons produced here may have ultraslow propagating velocity, and such solutions can be produced in a very small propagation distance of less than 1 cm with a single weak driving field with $\frac{1}{2}$ Rabi frequency, typically less than 100 MHz. Furthermore, the controllability of the present scheme allows us also to easily realize temporal Manakov solitons by actively adjusting the parameters of the system. Notice that scalar USOSs and soliton pairs in EIT media have been investigated recently [31–36,42,43]. The formation of the weak-light scalar spatial solitons, the two-component Thirring-type spatial solitons, and two-component vector temporal solitons have also been investigated in EIT-based systems [44–51]. However, until now there has been no study on three-component USOSs in optically dense media. Our results may lead to potential applications in optical information processing and engineering using multicomponent coupled solitons as the wavelength-division-multiplexed (WDM) channels or parallel-wavelength bits.

The article is arranged as follows. In the next section, we describe the theoretical model and investigate the dispersion properties of the system. In Sec. III, using reasonable and realistic approximate conditions, we derive the system's three coupled NLSEs, describing the envelope evolution of three probe fields. Then, three-component coupled soliton solutions with ultraslow group velocity in the system are provided, and their stability and controllability during propagation are discussed in detail. The Manakov temporal solitons in the tripod atomic system are also briefly discussed in this section. At the end of this article, we conclude with a brief summary in Sec. IV.

II. MODEL AND LINEARITY SOLUTION OF THE SYSTEM

Let us consider the five-level tripod atomic system shown in Fig. 1(a), in which three pulsed probe fields (a, b, c), with optical frequencies $\omega_{a,b,c}$ and $\frac{1}{2}$ Rabi frequencies $\Omega_{a,b,c}$, and a cw coherent couple field (d), with optical frequency ω_d and $\frac{1}{2}$ Rabi frequency Ω_d, complete their respective excitations. The electric-field vector for the probe and control fields can be written as $\vec{E}_{j=a,b,c} = \Sigma_j \vec{e}_j \mathcal{E}_j \exp[i(k_j z - \omega_j t)] + \text{c.c.}$ and $\vec{E}_d = \vec{e}_d \mathcal{E}_d \exp[i(k_d z - \omega_d t)] + \text{c.c.}$ $(j = a, b, c)$, where $k_{j,d}$, $\mathcal{E}_{j,d}$, and $e_{j,d}$ are wave vector, envelope amplitudes, and polarization direction of the jth probe or control fields, respectively. Figure 1(b) shows the corresponding possible arrangement of experimental apparatus. Under the electric-dipole and rotating-wave approximation, the density matrix equations of the system can be written as following

$$\dot{\rho}_{41} = id_{11}\rho_{41} + i\Omega_a(\rho_{11} - \rho_{44}) + i\Omega_b\rho_{21} + i\Omega_c\rho_{31} + i\Omega_d^*\rho_{51}, \quad (1)$$

$$\dot{\rho}_{51} = id_{12}\rho_{51} + i\Omega_d\rho_{41} - i\Omega_a\rho_{54}, \quad (2)$$

$$\dot{\rho}_{42} = id_{21}\rho_{42} + i\Omega_b(\rho_{22} - \rho_{44}) + i\Omega_d^*\rho_{52} + i\Omega_a\rho_{12} + i\Omega_c\rho_{32}, \quad (3)$$

$$\dot{\rho}_{52} = id_{22}\rho_{52} - i\Omega_b\rho_{54} + i\Omega_d\rho_{42}, \quad (4)$$

$$\dot{\rho}_{43} = id_{31}\rho_{43} + i\Omega_c(\rho_{33} - \rho_{44}) + i\Omega_a\rho_{13} + i\Omega_b\rho_{23} + i\Omega_d^*\rho_{53}, \quad (5)$$

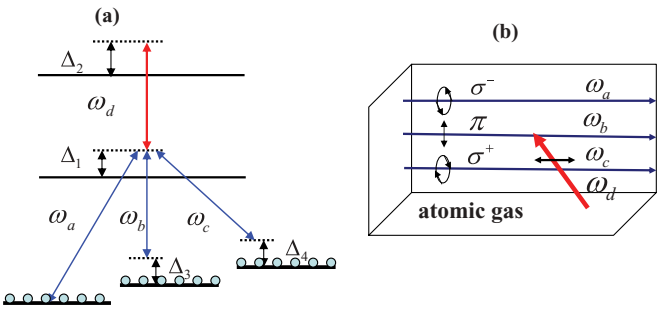

FIG. 1. (Color online) (a) Five-level tripod atomic system interacts with a cw coherent control laser (frequency ω_d and $\frac{1}{2}$ Rabi frequency Ω_d) and three pulsed probe fields (frequency $\omega_{a,b,c}$ and $\frac{1}{2}$ Rabi frequency $\Omega_{a,b,c}$). All the atoms are assumed to be initially prepared in the states $|1\rangle$, $|2\rangle$, and $|3\rangle$ with near amplitude as $\rho_{11} \simeq \rho_{22} \simeq \rho_{33} \simeq 1/3$. (b) Possible arrangement of experimental apparatus. The arrowhead represents the propagation direction of the fields; σ^-, π, and σ^+ represent the different polarized directions of the three weak probe fields; and ω_d represents the control field. The three weak fields are sent into the atomic medium to form three coupled ultraslow temporal optical solitons.

$$\dot{\rho}_{53} = id_{32}\rho_{53} + i\Omega_d\rho_{43} - i\Omega_c\rho_{54}, \quad (6)$$

$$\dot{\rho}_{21} = id_4\rho_{21} - i\Omega_a\rho_{24} + i\Omega_b^*\rho_{41}, \quad (7)$$

$$\dot{\rho}_{31} = id_5\rho_{31} - i\Omega_a\rho_{34} + i\Omega_c^*\rho_{41}, \quad (8)$$

$$\dot{\rho}_{32} = id_6\rho_{32} - i\Omega_b\rho_{34} + i\Omega_c^*\rho_{42}, \quad (9)$$

$$\dot{\rho}_{54} = id_7\rho_{54} + i\Omega_d(\rho_{44} - \rho_{55}) - i\Omega_a^*\rho_{51} - i\Omega_b^*\rho_{52} - i\Omega_c^*\rho_{53}, \quad (10)$$

and using the slowly varying envelope approximation, we obtain the following propagation equations for the three weak probe fields:

$$\frac{\partial\Omega_{a,b,c}}{\partial z} + \frac{1}{c}\frac{\partial\Omega_{a,b,c}}{\partial t} = i\kappa_{4j}\rho_{4j}, \quad (j = 1, 2, 3), \quad (11)$$

where $\rho_{ij} = \rho_{ji}^*$, $d_{11} = \Delta_1 + i(\gamma_{41} + \gamma_{42} + \gamma_{43})$, $d_{12} = \Delta_2 + i\gamma_{54}$, $d_{21} = \Delta_1 - \Delta_3 + i(\gamma_{41} + \gamma_{42} + \gamma_{43} + \gamma_{21})$, $d_{22} = \Delta_2 - \Delta_3 + i(\gamma_{54} + \gamma_{21})$, $d_{31} = \Delta_1 - \Delta_4 + i(\gamma_{41} + \gamma_{42} + \gamma_{43} + \gamma_{31} + \gamma_{32})$, $d_{32} = \Delta_2 - \Delta_4 + i(\gamma_{54} + \gamma_{31} + \gamma_{32})$, $d_4 = \Delta_3 + i\gamma_{21}$, $d_5 = \Delta_4 + i(\gamma_{31} + \gamma_{32})$, $d_6 = \Delta_4 - \Delta_3 + i(\gamma_{31} + \gamma_{32} + \gamma_{21})$, and $d_7 = \Delta_2 - \Delta_1 + i(\gamma_{41} + \gamma_{42} + \gamma_{43} + \gamma_{54})$. Decay rates γ_{ij} are included phenomenologically in these equations, and the propagation coefficients are defined by $\kappa_{4j} = N_a\omega_j|\mu_{4j}|^2/(2\hbar\varepsilon_0 c)$ with N_a, μ_{4j}, c, and ε_0 being atomic density, dipole moment for the transition $|4\rangle \to |j\rangle$, velocity of light in vacuum, and vacuum dielectric constant, respectively. Here, the system was considered as a closed system. Alone with the density matrix equations, we also have the population conservation law $\rho_{11} + \rho_{22} + \rho_{33} + \rho_{44} + \rho_{55} \simeq 1$. $\Delta_1 = \omega_a - \epsilon_4$ is the one-photon detuning, whereas $\Delta_2 = \omega_a + \omega_d - \epsilon_5$, $\Delta_3 = \omega_a - \omega_b - \epsilon_2$, and $\Delta_4 = \omega_a - \omega_c - \epsilon_3$ are the two-photon detunings between $|1\rangle \to |5\rangle$, $|1\rangle \to |2\rangle$, and $|1\rangle \to |3\rangle$, respectively, where ϵ_j is the energy of state $|j\rangle$ $(\epsilon_1 = 0)$.

In order to provide a clear picture of the interplay between the dispersion and nonlinear effects of the atomic system interacting with four optical fields, we must solve the coupled equations (1)–(11). Before solving those nonlinearly coupled

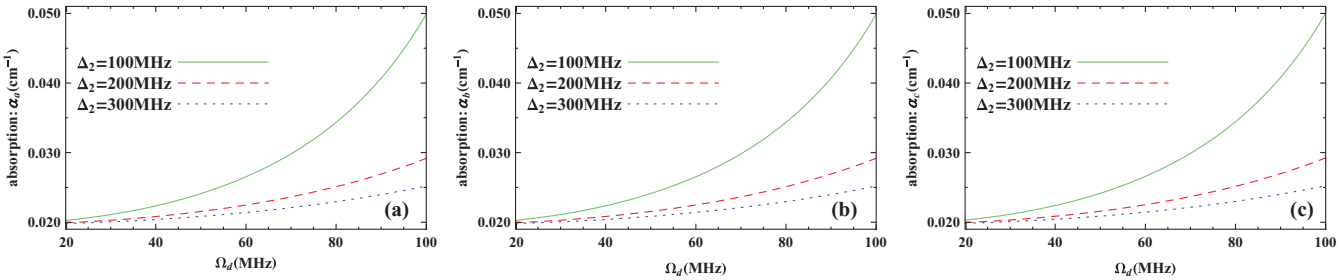

FIG. 2. (Color online) Absorption coefficients α_a (a), α_b (b), and α_c (c) of the three pulsed probe fields versus the dimensionless $\frac{1}{2}$ Rabi frequency $\Omega_d\tau_0$ for several different two-photon detunings $\Delta_2\tau_0$ with the parameters $(\gamma_{41}+\gamma_{42}+\gamma_{43})\tau_0 = 0.053$, $\gamma_{31}\tau_0 = \gamma_{32}\tau_0 = \gamma_{21}\tau_0 = 6\times10^{-5}$, $\gamma_{54}\tau_0 = 0.69\times10^{-2}$, $\kappa_{41}\tau_0 = \kappa_{42}\tau_0 = \kappa_{43}\tau_0 = 10\ \mathrm{cm}^{-1}$, $\Delta_1\tau_0 = 3$, $\Delta_3\tau_0 = -1\times10^{-3}$, and $\Delta_4\tau_0 = -5\times10^{-4}$.

equations, let us first examine the linear excitations of the system, which may provide useful hints of the weak nonlinear theory developed in the next section. To this end, we assume that the Rabi frequencies $\Omega_{a,b,c}$ of the pulsed probe fields are much smaller than that of the control field Ω_d, and all the atoms are assumed to be prepared in the states $|1\rangle$, $|2\rangle$, and $|3\rangle$ with approximately equal populations (i.e., $\rho_{11}\simeq\rho_{22}\simeq\rho_{33}\simeq\frac{1}{3}$) whereas $\rho_{44}\simeq\rho_{55}\simeq0$.[1] In the low-density approximation and by adiabatically eliminating the atomic degrees of freedom, the perturbation approach can be applied to the atomic part, which is introduced in terms of perturbation expansion $\rho_{ij}=\Sigma_k\rho_{ij}^{(k)}$, where $\rho_{ij}^{(k)}$ is the kth order part of ρ_{ij} in terms of $\Omega_{a,b,c}$, and it can be shown that $\rho_{ij}^{(0)}=0(i\neq j)$ and $\rho_{44}^{(k)}=\rho_{55}^{(k)}=0$. By considering the first order of the pulsed probe fields and taking the temporal Fourier transform of Eqs. (1)–(11), we obtain

$$\rho_{jk}^{(1)}(t)=\frac{1}{\sqrt{2\pi}}\int_{-\infty}^{\infty}\beta_{jk}^{(1)}(\omega)e^{-i\omega t}d\omega,\quad j{=}k{=}1,2,3,4,5, \tag{12}$$

$$\Omega_k(t)=\frac{1}{\sqrt{2\pi}}\int_{-\infty}^{\infty}\Lambda_k(\omega)e^{-i\omega t}d\omega,\quad k=a,b,c. \tag{13}$$

Then, with ω being the Fourier transform variable, we have

$$\beta_{21}^{(1)}=\beta_{31}^{(1)}=\beta_{32}^{(1)}=\beta_{54}^{(1)}=0, \tag{14}$$

$$\beta_{41}^{(1)}=\frac{(\omega+d_{12})\Omega_a}{3D_1(\omega)}, \tag{15}$$

$$\beta_{42}^{(1)}=\frac{(\omega+d_{22})\Omega_b}{3D_2(\omega)}, \tag{16}$$

$$\beta_{43}^{(1)}=\frac{(\omega+d_{32})\Omega_c}{3D_3(\omega)}, \tag{17}$$

$$\beta_{51}^{(1)}=\frac{-\Omega_d\Omega_a}{3D_1(\omega)},\quad \beta_{52}^{(1)}=\frac{-\Omega_d\Omega_b}{3D_2(\omega)},\quad \beta_{53}^{(1)}=\frac{-\Omega_d\Omega_c}{3D_3(\omega)}, \tag{18}$$

$$\frac{\partial\Lambda_{a,b,c}}{\partial z}+\frac{\omega}{c}\frac{\partial\Lambda_{a,b,c}}{\partial t}=i\kappa_{4j}\beta_{4j}^{(1)}\quad(j=1,2,3), \tag{19}$$

where $D_1(\omega)=|\Omega_d|^2-(\omega+d_{12})(\omega+d_{11})$, $D_2(\omega)=|\Omega_d|^2-(\omega+d_{22})(\omega+d_{21})$, and $D_3(\omega)=|\Omega_d|^2-(\omega+d_{32})(\omega+d_{31})$. Here β_{ij} and $\Lambda_{a,b,c}$ are the Fourier transforms of ρ_{ij} and $\Omega_{a,b,c}$, respectively. With the help of Eqs. (14)–(18), Eq. (19) can be solved analytically, yielding

$$\Lambda_{j=a,b,c}(z,\omega)=\Lambda_j(0,\omega)\exp[iK_j(\omega)z], \tag{20}$$

where $K_a(\omega)$, $K_b(\omega)$, and $K_c(\omega)$ are three branches of the linear dispersion relation for the linear excitations corresponding to the three pulse probe fields Ω_a, Ω_b, and Ω_c, respectively. In most operation conditions, they can be expanded into a rapid conversion power series around the center frequencies $\omega_{a,b,c}$ of the pulse probe fields; that is, $\omega=0$. We thus have

$$K_a(\omega)=\frac{\omega}{c}+\kappa_{41}\frac{\omega+d_{12}}{3D_1(\omega)}, \tag{21}$$

$$K_b(\omega)=\frac{\omega}{c}+\kappa_{42}\frac{\omega+d_{22}}{3D_2(\omega)}, \tag{22}$$

$$K_c(\omega)=\frac{\omega}{c}+\kappa_{43}\frac{\omega+d_{32}}{3D_3(\omega)}, \tag{23}$$

with $K_j(\omega)=K_j+K_j'\omega+K_j''\omega^2+\cdots$ (the detailed expressions of K_j, K_j', and K_j'' can be found in Appendix A). The physical interpretation of the dispersion coefficients in Eqs. (21)–(23) is rather clear. $K_{j=a,b,c}=\phi_{j=a,b,c}+i\alpha_{j=a,b,c}$ describes the phase shift $\phi_{j=a,b,c}$ per unit length and absorption coefficient $\alpha_{j=a,b,c}$ of the pulsed probe fields, $K'_{j=a,b,c}$ gives the group velocities $V_{gj=ga,gb,gc}=\mathrm{Re}[1/K'_{j=a,b,c}]$, and $K''_{j=a,b,c}$ represents the group velocity dispersion that contributes to the shape change of laser pulses. Figure 2 plots the absorption coefficients $\alpha_{j=a,b,c}$ of the three pulsed probe fields versus the dimensionless $\frac{1}{2}$ Rabi frequency $\Omega_d\tau_0$ for several different two-photon detuning $\Delta_2\tau_0$. The amplitudes of absorption coefficients in Fig. 2 are on the order of 10^{-2} cm^{-1}, and the absorption of the three pulsed probe fields can be almost simultaneously suppressed because of the contributions of one control field under appropriate conditions in this five-level tripod atomic system. For $\tau_0=1\times10^{-8}$ s, with the same parameter setting as in Fig. 2, we also demonstrate the dependence of the group velocities for the three pulsed probe fields in Fig. 3, which shows that the group velocities are much slower than the light velocity in a vacuum (i.e., $V_{gj}/c\sim10^{-3}$). Here, we also emphasize that the three-component coupled solitons produced in this way generally travel with group velocities given by $V_{ga}=1/K'_a$, $V_{gb}=1/K'_b$, and

[1]It is not necessary to start with equal populations in the three states $|1\rangle$, $|2\rangle$, and $|3\rangle$ initially. Even though the initial populations in these three states with less difference will lead to the mismatch of group velocity, solitons can still form by shifting their frequencies (detunings).

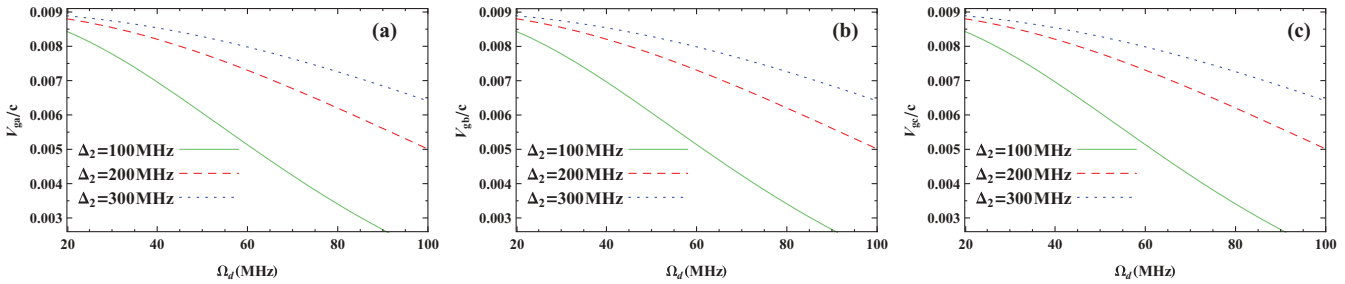

FIG. 3. (Color online) Relative group velocities V_{ga}/c (a), V_{gb}/c (b), and V_{gc}/c (c) of the three pulsed probe fields versus the dimensionless $\frac{1}{2}$ Rabi frequency $\Omega_d\tau_0$ for $\tau_0 = 1 \times 10^{-8}$ s, with the other parameters being the same as in Fig. 2.

$V_{gc} = 1/K_c'$, respectively, which are nearly matched under appropriate parameter conditions as shown in Fig. 3.

It should be noted that Eq. (19) is obtained in the linear regime of the system under the weak-field and adiabatic approximations while ignoring the higher order terms of probe fields. In order to preserve the shapes of the three probe fields, we need to include the Kerr-type SPM and CPM, which may balance the spread effect due to the group velocity dispersion described by the $K''_{a,b,c}$ coefficients to generate the three-component coupled solitons of the probe fields. In the next section, we explore the higher order terms of $\Omega_{a,b,c}$ while systematically keeping terms up to ω^2 in Eqs. (21)–(23) for the purpose of demonstrating the formation of ultraslow temporal coupled optical solitons in the five-level tripod atomic system.

III. NONLINEAR DYNAMICS AND THE THREE-COMPONENT COUPLED SOLITONS

With the dispersion coefficients in hand, we now investigate the nonlinear evolution of the three probe fields including the Kerr-type SPM and CPM, which may balance the spread effect due to the group velocity dispersion. We explore the higher order $\Omega_{a,b,c}$ by systematically keeping terms up to ω^2 in Eqs. (21)–(23) and show that a reasonable and realistic set of parameters can be found so that the SPM and CPM effects can precisely balance group velocity dispersion in the ultraslow propagation regime. This leads to Eq. (11), describing the propagation of the three pulse probe fields that evolve into three coupled NLSEs, which admit solutions describing three-component coupled optical solitons. Following the method developed in Refs. [31–33], we take a trial function $\Lambda_{j=a,b,c}(z,\omega) = \Lambda_{j=a,b,c}(z,\omega)\exp[izK_{j=a,b,c}]$ and substitute it into the wave equation

$$\frac{\partial}{\partial z}\Lambda_j(z,\omega) = iK_j(\omega)\Lambda_j(z,\omega), \quad j = a,b,c. \tag{24}$$

We then obtain

$$\frac{\partial\Lambda_j(z,\omega)}{\partial z}e^{izK_j} = i(K'_j\omega + K''_j\omega^2)\Lambda_j(z,\omega)e^{izK_j}, \quad j = a,b,c. \tag{25}$$

Here we only keep terms up to order ω^2 when expanding the propagation constant $K_{j=a,b,c}$. In order to balance the interplay between the group velocity dispersion and the nonlinear effect, it is necessary for us to consider the higher order terms in the probe field amplitude, namely, the nonlinear terms on the right-hand side of Eq. (11):

$$i\kappa_{41} \simeq i\kappa_{41}\rho_{41}^{(1)} + iT_a^{\rm nl}, \tag{26}$$

$$i\kappa_{42} \simeq i\kappa_{42}\rho_{42}^{(1)} + iT_b^{\rm nl}, \tag{27}$$

$$i\kappa_{43} \simeq i\kappa_{43}\rho_{43}^{(1)} + iT_c^{\rm nl}, \tag{28}$$

where the third-order nonlinear term $T^{\rm nl}_{j=a,b,c}$ is given by

$$T_a^{\rm nl} = -\kappa_{41}e^{-izK_a}\frac{\rho_{32}^{(2)}d_{12}\Omega_c - \rho_{21}^{(2)}d_{12}\Omega_a - \rho_{54}^{(2)}\Omega_a\Omega_d^*}{-d_{11}d_{12} + |\Omega_d|^2}, \tag{29}$$

$$T_b^{\rm nl} = -\kappa_{42}e^{-izK_b}\frac{\rho_{32}^{(2)}d_{22}\Omega_c - \rho_{21}^{(2)}d_{22}\Omega_a - \rho_{54}^{(2)}\Omega_b\Omega_d^*}{-d_{21}d_{22} + |\Omega_d|^2}, \tag{30}$$

$$T_c^{\rm nl} = -\kappa_{43}e^{-izK_c}\frac{-\rho_{31}^{(2)}d_{32}\Omega_a - \rho_{32}^{(2)}d_{32}\Omega_b - \rho_{54}^{(2)}\Omega_c\Omega_d^*}{-d_{31}d_{32} + |\Omega_d|^2}, \tag{31}$$

with $\rho_{21}^{(2)}$, $\rho_{31}^{(2)}$, $\rho_{54}^{(2)}$, and $\rho_{32}^{(2)}$ given by

$$\rho_{21}^{(2)} = -\frac{\Omega_a^*\rho_{42}^{(1)} + \Omega_b^*\rho_{41}^{(1)}}{d_4}, \tag{32}$$

$$\rho_{31}^{(2)} = -\frac{\Omega_a^*\rho_{43}^{(1)} + \Omega_c^*\rho_{41}^{(1)}}{d_5}, \tag{33}$$

$$\rho_{32}^{(2)} = -\frac{\Omega_b^*\rho_{43}^{(1)} + \Omega_c^*\rho_{42}^{(1)}}{d_6}, \tag{34}$$

$$\rho_{54}^{(2)} = \frac{\Omega_a^*\rho_{51}^{(1)} + \Omega_b^*\rho_{52}^{(1)} + \Omega_c^*\rho_{53}^{(1)}}{d_7}, \tag{35}$$

where $\rho_{41}^{(1)}$, $\rho_{42}^{(1)}$, $\rho_{43}^{(1)}$, $\rho_{51}^{(1)}$, $\rho_{52}^{(1)}$, and $\rho_{53}^{(1)}$ can be obtained from Eqs. (14)–(18); that is, $\rho_{41}^{(1)} = d_{12}\Omega_a/3D_1(0)$, $\rho_{42}^{(1)} = d_{22}\Omega_b/3D_2(0)$, $\rho_{43}^{(1)} = d_{32}\Omega_c/3D_3(0)$, $\rho_{51}^{(1)} = -\Omega_d\Omega_a/3D_1(0)$, $\rho_{52}^{(1)} = -\Omega_d\Omega_b/3D_2(0)$, and $\rho_{53}^{(1)} = -\Omega_d\Omega_c/3D_3(0)$.

With the help of nonlinear terms in Eqs. (29)–(31), we now turn to the investigation of the nonlinear dynamics of the five-level tripod atomic system. By taking the inverse Fourier transform of Eq. (25),

$$\Omega_k(z,t) = \frac{1}{\sqrt{2\pi}}\int_{-\infty}^{\infty}\Lambda_k(z,\omega)e^{-i\omega t}d\omega, \quad k = a,b,c, \tag{36}$$

the nonlinear wave equations, namely the coupled NLSEs, that govern the evolution of the slowly varying envelopes $\Omega_a(z,t)$, $\Omega_b(z,t)$, and $\Omega_c(z,t)$, can be obtained by

$$-i\left(\frac{\partial}{\partial z}+\frac{1}{V_{gj}}\frac{\partial}{\partial t}\right)\Omega_j+iK_j''\frac{\partial^2}{\partial t^2}\Omega_j=T_j^{\rm nl},\quad j=a,b,c, \tag{37}$$

where $V_{gj}=\mathrm{Re}[1/K_j']$ describes the group velocity and K_j'' describes the group velocity dispersion. By substituting Eqs. (29)–(31) into Eq. (37), we can rewrite Eq. (37) as

$$\begin{aligned}&-i\left(\frac{\partial}{\partial z}+\frac{1}{V_{ga}}\frac{\partial}{\partial t}\right)\Omega_a+iK_a''\frac{\partial^2}{\partial t^2}\Omega_a\\&=(U_{aa}e^{-\alpha_a z}|\Omega_a|^2+U_{ab}e^{-\alpha_b z}|\Omega_b|^2+U_{ac}e^{-\alpha_c z}|\Omega_c|^2)\Omega_a,\end{aligned} \tag{38}$$

$$\begin{aligned}&-i\left(\frac{\partial}{\partial z}+\frac{1}{V_{gb}}\frac{\partial}{\partial t}\right)\Omega_b+iK_b''\frac{\partial^2}{\partial t^2}\Omega_b\\&=(U_{ba}e^{-\alpha_a z}|\Omega_a|^2+U_{bb}e^{-\alpha_b z}|\Omega_b|^2+U_{bc}e^{-\alpha_c z}|\Omega_c|^2)\Omega_b,\end{aligned} \tag{39}$$

$$\begin{aligned}&-i\left(\frac{\partial}{\partial z}+\frac{1}{V_{gc}}\frac{\partial}{\partial t}\right)\Omega_c+iK_c''\frac{\partial^2}{\partial t^2}\Omega_c\\&=(U_{ca}e^{-\alpha_a z}|\Omega_a|^2+U_{cb}e^{-\alpha_b z}|\Omega_b|^2+U_{cc}e^{-\alpha_c z}|\Omega_c|^2)\Omega_c,\end{aligned} \tag{40}$$

where absorption coefficients $\alpha_j=\mathrm{Im}[K_j]$, as illustrated in Fig. 2 with different parameter values, are given by

$$\alpha_a=\mathrm{Im}\left[\kappa_{41}\frac{d_{12}}{3(|\Omega_d|^2-d_{12}d_{11})}\right], \tag{41}$$

$$\alpha_b=\mathrm{Im}\left[\kappa_{42}\frac{d_{22}}{3(|\Omega_d|^2-d_{22}d_{21})}\right], \tag{42}$$

$$\alpha_c=\mathrm{Im}\left[\kappa_{43}\frac{d_{32}}{3(|\Omega_d|^2-d_{32}d_{31})}\right], \tag{43}$$

and the nonlinear coefficients U_{aa}, U_{bb} and U_{cc}, U_{ab}, U_{ba}, U_{ac}, U_{ca}, U_{bc}, U_{cb}, which characterize SPM and CPM respectively of the three pulse probe fields, are given by

$$U_{aa}=\kappa_{41}\frac{d_{12}\left(\gamma_{54}^2+\Delta_2^2+|\Omega_d|^2\right)}{27(|\Omega_d|^2-d_{12}d_{11})(|\Omega_d|^2-d_{12}d_{11})^2}, \tag{44}$$

$$U_{ab}=\kappa_{41}\frac{d_{12}[(\gamma_{21}+\gamma_{54})^2+(\Delta_2-\Delta_3)^2+|\Omega_d|^2]}{27(|\Omega_d|^2-d_{12}d_{11})(|\Omega_d|^2-d_{22}d_{21})^2}, \tag{45}$$

$$U_{ac}=\kappa_{41}\frac{d_{12}[(\gamma_{31}+\gamma_{32}+\gamma_{54})^2+(\Delta_2-\Delta_4)^2+|\Omega_d|^2]}{27(|\Omega_d|^2-d_{12}d_{11})(|\Omega_d|^2-d_{32}d_{31})^2}, \tag{46}$$

$$U_{ba}=\kappa_{42}\frac{d_{22}\left(\gamma_{54}^2+\Delta_2^2+|\Omega_d|^2\right)}{27(|\Omega_d|^2-d_{22}d_{21})(|\Omega_d|^2-d_{12}d_{11})^2}, \tag{47}$$

$$U_{bb}=\kappa_{42}\frac{d_{22}[(\gamma_{21}+\gamma_{54})^2+(\Delta_2-\Delta_3)^2+|\Omega_d|^2]}{27(|\Omega_d|^2-d_{22}d_{21})(|\Omega_d|^2-d_{22}d_{21})^2}, \tag{48}$$

$$U_{bc}=\kappa_{42}\frac{d_{22}[(\gamma_{31}+\gamma_{32}+\gamma_{54})^2+(\Delta_2-\Delta_4)^2+|\Omega_d|^2]}{27(|\Omega_d|^2-d_{22}d_{21})(|\Omega_d|^2-d_{32}d_{31})^2}, \tag{49}$$

$$U_{ca}=\kappa_{43}\frac{d_{32}\left(\gamma_{54}^2+\Delta_2^2+|\Omega_d|^2\right)}{27(|\Omega_d|^2-d_{32}d_{31})(|\Omega_d|^2-d_{12}d_{11})^2}, \tag{50}$$

$$U_{cb}=\kappa_{43}\frac{d_{32}[(\gamma_{21}+\gamma_{54})^2+(\Delta_2-\Delta_3)^2+|\Omega_d|^2]}{27(|\Omega_d|^2-d_{32}d_{31})(|\Omega_d|^2-d_{22}d_{21})^2}, \tag{51}$$

$$U_{cc}=\kappa_{43}\frac{d_{32}[(\gamma_{31}+\gamma_{32}+\gamma_{54})^2+(\Delta_2-\Delta_4)^2+|\Omega_d|^2]}{27(|\Omega_d|^2-d_{32}d_{31})(|\Omega_d|^2-d_{32}d_{31})^2}. \tag{52}$$

Equations (38)–(40) have complex coefficients and generally do not allow soliton solutions. However, because of the contribution of the control field, the absorptions of the three pulsed probe fields can be almost simultaneously suppressed under appropriate conditions, which leads to $\exp(-\alpha_j L)\simeq 1$ with L being the length of atomic system. Furthermore, we show for the present system that practical parameters can be found so that the imaginary parts of the complex coefficients are much smaller than the corresponding real parts, that is, $K''_{j=a,b,c}=K''_{jr}+iK''_{ji}\simeq K''_{jr}$ $(j=a,b,c)$, $U_{lmn}=U_{lmr}+iU_{lmi}\simeq U_{lmr}$ $(l,m=a,b,c)$, $U_{aar}=U_{bar}=U_{car}=W_a$, $U_{abr}=U_{bbr}=U_{cbr}=W_b$, and $U_{acr}=U_{bcr}=U_{ccr}=W_c$. If we define $\tau=(t-z/V_{ga})/\tau_0$, $\delta_{aj}=(V_{ga}-V_{gj})/V_{g1}V_{gj}$, $\xi=z/L_{Da}$, $L_{Da}=\tau_0^2/|K''_{ar}|$, $\Omega_j(t,z)=F_{0j}u_j(\tau,\xi)$, $L_{\mathrm{nl}j}=1/(|W_j||F_{0j}|^2)$ (characterizing the nonlinear length), $L_{Dj}=\tau_0^2/|K''_{jr}|$ (characterizing the dispersion length), and $L_{\delta j}=\tau_0/|\delta_{aj}|$ (characterizing the walk-off length) with τ_0, F_{0j} being the pulse width and amplitudes of the three pulsed probe fields, the nonlinear evolution equations (38)–(40) can be simplified in the dimensionless forms as

$$\begin{aligned}&i\left(\frac{\partial}{\partial\xi}+G_{\delta a}\frac{\partial}{\partial\tau}\right)u_a-G_a\frac{\partial^2}{\partial\tau^2}u_a-(p_{aa}|u_a|^2\\&\quad+p_{ba}|u_b|^2+p_{ca}|u_c|^2)u_a=0,\end{aligned} \tag{53}$$

$$\begin{aligned}&i\left(\frac{\partial}{\partial\xi}+G_{\delta b}\frac{\partial}{\partial\tau}\right)u_b-G_b\frac{\partial^2}{\partial\tau^2}u_b-(p_{bb}|u_b|^2\\&\quad+p_{ab}|u_a|^2+p_{cb}|u_c|^2)u_a=0,\end{aligned} \tag{54}$$

$$\begin{aligned}&i\left(\frac{\partial}{\partial\xi}+G_{\delta c}\frac{\partial}{\partial\tau}\right)u_c-G_c\frac{\partial^2}{\partial\tau^2}u_c-(p_{cc}|u_c|^2\\&\quad+p_{ac}|u_a|^2+p_{bc}|u_b|^2)u_b=0,\end{aligned} \tag{55}$$

where we have set $L_{Dj}=L_{\mathrm{NL}j}$ $(j=a,b,c)$, which means the well balance between the group velocity dispersion and nonlinear effects in our system. Thus, we have $F_{0j}=1/\tau_0|K''_{jr}/W_j|^{1/2}$, $G_{\delta j}=\delta_{aj}L_{Da}/\tau_0$, $G_j=K''_{jr}/|K''_{ar}|$, $p_{jj}=W_j/|W_j|$, and $p_{mj}=W_m/|W_j|$. A major obstacle for the formation of three-component coupled optical solitons is the group-velocity mismatch $G_{\delta j}$ that appears in equations (53)–(55). In the absence of the CPM nonlinear effects, the three probe fields separate individually or move away from each other after propagating a distance known as the "walk-off" length $L_{\delta j}$, resulting from the group-velocity mismatch [15]. However, solitons can shift their frequencies (wavelengths) in such a way that the faster moving pulse slows down while the slower moving pulse speeds up, so that the three pulses continue to overlap indefinitely, which is the main mechanism in the previous investigations used to generate vector optical solitons under a group-velocity mismatch. In order to find the soliton solutions of Eqs. (53)–(55), we assume

the solutions in the form of

$$u_a(\xi,\tau) = U_a(\xi,\tau)\exp(i\vartheta_a\xi - iM_a\tau), \quad (56)$$

$$u_b(\xi,\tau) = U_b(\xi,\tau)\exp(i\vartheta_b\xi - iM_b\tau), \quad (57)$$

$$u_c(\xi,\tau) = U_c(\xi,\tau)\exp(i\vartheta_c\xi - iM_c\tau), \quad (58)$$

with the carrier-frequency shifts $M_j = G_{\delta j=a,b,c}/(2G_{j=a,b,c})$ and $\lambda_{j=a,b,c} = \vartheta_{j=a,b,c} - G^2_{\delta j=a,b,c}/(4G_{j=a,b,c})$. Consequently, $U_{j=a,b,c}$ satisfies the ordinary differential equations

$$G_a\frac{\partial^2}{\partial\tau^2}U_a + (p_{aa}|U_a|^2 + p_{ba}|U_b|^2 + p_{ca}|U_c|^2)U_a - \lambda_a U_a = 0, \quad (59)$$

$$G_b\frac{\partial^2}{\partial\tau^2}U_b + (p_{bb}|U_b|^2 + p_{ab}|U_a|^2 + p_{cb}|U_c|^2)U_b - \lambda_b U_b = 0, \quad (60)$$

$$G_c\frac{\partial^2}{\partial\tau^2}U_c + (p_{cc}|U_c|^2 + p_{ac}|U_a|^2 + p_{bc}|U_b|^2)U_c - \lambda_c U_c = 0. \quad (61)$$

This transformation of Eqs. (56)–(58) has removed the group velocity mismatched term $G_{\delta j=a,b,c}$ from the evolution and transferred it into carrier-frequency (wavelength) shifts of each individual pulsed probe field. The three coupled equations (59)–(61) are the simplest coupled NLSEs, that is, the incoherent coupled NLSEs, which admit exact solutions under certain conditions [52,53].

We give a practical example to show that a set of experimentally achievable parameters of our five-level tripod atomic system can be found to support three-component coupled USOSs. We consider cold ^{87}Rb atoms with the designed states chosen as mentioned previously, for example, $5S_{1/2}, F = 1, M_F = -1, 0, 1$ as $|1\rangle$, $|2\rangle$, $|3\rangle$, respectively, and $5P_{1/2}, F = 1, M_F = 0$, $5D_{3/2}, F = 2$ as $|4\rangle$ and $|5\rangle$, respectively. The corresponding decay rates are $(\gamma_{41}+\gamma_{42}+\gamma_{43})\tau_0 = 0.053$, $\gamma_{54}\tau_0 = 0.69\times10^{-2}$, and $\gamma_{31}\tau_0 = \gamma_{32}\tau_0 = \gamma_{21}\tau_0 = 6\times10^{-5}$ [54]. We have neglected the decay ($|4\rangle \to 5S_{1/2}, F = 2$) because of their small effect [54]; thus, the system can be considered as a closed system. Taking $\kappa_{41}\tau_0 \simeq \kappa_{42}\tau_0 \simeq \kappa_{43}\tau_0 \simeq 10$ cm^{-1}, $\Omega_d\tau_0 = 0.9$, $\Delta_1\tau_0 = 3$, $\Delta_2\tau_0 = 1$, $\Delta_3\tau_0 = -1\times10^{-3}$, and $\Delta_4\tau_0 = -5\times10^{-4}$, we can obtain $K'_a \simeq (1.254 - 0.075i)\times10^{-8}$ s cm^{-1}, $K'_b \simeq (1.252 - 0.075i)\times10^{-8}$ s cm^{-1}, $K'_c \simeq (1.253 - 0.075i)\times10^{-8}$ s cm^{-1}, $K''_a \simeq (-1.595 + 0.138i)\times10^{-16}$ s^2 cm^{-1}, $K''_b \simeq (-1.588 + 0.138i)\times10^{-16}$ s^2 cm^{-1}, $K''_c \simeq (-1.591 + 0.138i)\times10^{-16}$ s^2 cm^{-1}, $U_{aa} \simeq U_{ba} \simeq U_{ca} = W_a \simeq (-5.462 + 0.023i)\times10^{-17}$ s^2 cm^{-1}, $U_{ab} \simeq U_{bb} \simeq U_{cb} = W_b \simeq (-5.448 + 0.023i)\times10^{-17}$ s^2 cm^{-1}, $U_{ac} \simeq U_{bc} \simeq U_{cc} = W_c \simeq (-5.457 + 0.023i)\times10^{-17}$ s^2 cm^{-1}, and $\alpha_a \simeq \alpha_b \simeq \alpha_c \simeq 0.041$ cm^{-1}. Clearly, for all complex coefficients, the imaginary parts are indeed much smaller than their corresponding real parts. The physical reason for such small imaginary parts is the quantum interference effect produced by the cw coherent control field Ω_d. With this set of parameters, we have the ultraslow group velocity, that is, $V_{ga}/c \simeq 2.658\times10^{-3}$, $V_{gb}/c \simeq 2.662\times10^{-3}$, and $V_{gc}/c \simeq 2.660\times10^{-3}$. Choosing the pulse width $\tau_0 = 1\times10^{-8}$ s, we can obtain $L_{Da} = L_{\mathrm{nl}a} = 0.627$ cm, $L_{Db} = L_{\mathrm{nl}b} = 0.630$ cm, $L_{Dc} = L_{\mathrm{nl}c} = 0.629$ cm, $F_{0a} \simeq F_{0b} \simeq F_{0c} \simeq U_0 \simeq 58$ MHz, and the dimensionless coefficients $G_a \simeq -1$, $G_b \simeq -0.996$, $G_c \simeq -0.998$, $G_{\delta a} = 0$, $G_{\delta b} \simeq -1.25\times10^{-3}$, $G_{\delta c} \simeq -0.63\times10^{-3}$, $p_{aa} = p_{bb} = p_{cc} = -1$, $p_{ba} \simeq -0.998$, $p_{ca} \simeq -0.999$, $p_{ab} \simeq -1.003$, $p_{cb} \simeq -1.001$, $p_{ac} \simeq -1.001$, and $p_{bc} \simeq -0.999$. By introducing the normalizing coefficients, we have defined the central channel by $j = a$ and used it as a reference channel so that $G_a/\lambda_a = p_{aa}/\lambda_a = -1$. By renormalizing $\sqrt{\lambda_a}\tau \to \tau$, we rewrite Eqs. (59)–(61) in the form

$$\frac{\partial^2 U_a}{\partial\tau^2} + \left(|U_a|^2 + \sum_{n\neq a} p_{la}|U_n|^2\right)U_a - U_a = 0, \quad (62)$$

$$G_n\frac{\partial^2 U_n}{\partial\tau^2} + \left(p_{nj}|U_n|^2 + \sum_{l\neq n} p_{lj}|U_m|^2\right)U_n - \lambda_n U_n = 0, \quad (63)$$

where G_n, $p_{lj,nj}$, and λ_n are rescaled as $G_n = G_j/\lambda_a$, $p_{nj} = p_{jj}/\lambda_a$, $p_{lj} = p_{mj}/\lambda_a$, and $\lambda_n = \lambda_j/\lambda_a$, respectively.

We now present numerical examples to demonstrate the existence of three-coupled USOSs in the system. By assuming that in the presence of CPM all components of the soliton have the same "sech" shape, that is, $U_n(\tau) = A_n\mathrm{sech}(\tau)$, and substituting this solution in Eqs. (62) and (63), the amplitudes A_n are found to satisfy the set of coupled algebraic equations $A_a^2 + \sum_{n=b} p_n A_n^2 = 2$ and $p_n A_n^2 + \sum_{l\neq n} p_l A_l^2 = 2G_n$. Based on the previously mentioned parameter settings, we show in Fig. 4 the numerical solutions to Eqs. (62) and (63) with complex coefficients by an iteration method. Our simulations show the three fields have the same hyperbolic secant shape and confirm the conclusion that USOSs can form in the present system. Because all parameters G_n and p_{nj} in Eqs. (62) and (63) are very close to -1 and the group velocity of the three pulsed probe fields is nearly matched with a very small differences in a wide range (as shown in Fig. 3), our numerical solution describes three-component coupled bright solitons with nearly equal intensity, as illustrated in Fig. 4. We should

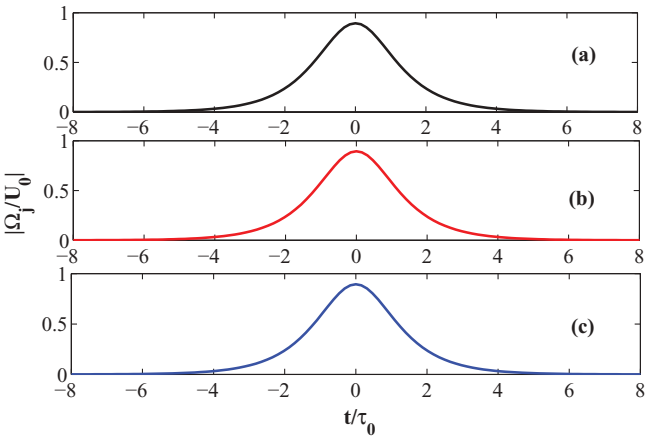

FIG. 4. (Color online) $|\Omega_j/U_0|$ [(a) $|\Omega_a/U_0|$, (b) $|\Omega_b/U_0|$, (c) $|\Omega_c/U_0|$] as the function of the dimensionless time t/τ_0 obtained by numerically integrating Eqs. (62) and (63). All the parameters are present in the main text.

mentioned that the special case in which the SPM and CPM nonlinear terms in the set of Eqs. (59)–(61) of three coupled NLSEs are exactly equal ($p_{jj} = p_{mj} = -1$) corresponds to a three-component generalization of the Manakov model for the optical solitons [16]. In this special case, Eqs. (59)–(61) are known to possess exact three-component solitons [55,56].

IV. DISCUSSION AND CONCLUSION

In order to further demonstrate the formation and evolution of the three-component coupled ultraslow temporal optical solitons in the present system and check their stabilities, we show in Fig. 5 the analytical solutions of Eqs. (62)–(63) (dashed lines) and the full numerical solutions (solid lines) obtained by directly integrating Eqs. (1)–(11) without using any approximations. The initial conditions used in the numerical calculations are $z = 0$ and $t = 0$, $\Omega_a(0,t)/U_0 = \Omega_b(0,t)/U_0 = \Omega_c(0,t)/U_0 = \mathrm{sech}(2t/\tau_0)$. In Fig. 5, each curve contains three distinguishable traces, representing the perfectly matched solitons. We note that the dotted lines are numerical solutions without including nonlinear terms (the SPM and CPM effects), which exhibit severe pulse spreading, as expected. We emphasis that we have neglected the contributions of the time derivatives (i.e., $\partial/\partial t$) in deriving the nonlinear term U_{ij}. These contributions, however, can lead to significant propagation effects at large propagation distances (i.e., giving an additional group velocity correction). Therefore, the analytical solutions and the numerical solutions will gradually separate. Besides, our numerical calculations show that it is not necessary to start with three exactly matched $\mathrm{sech}(t/\tau_0)$ functions. By taking three matched Gaussian inputs, the shapes of fields have a full width at half maximum that is about 18% larger than the initial hyperbolic pulse shape used in the previous simulation. Figure 6 shows the evolution of the input signal fields at $z = 0.8$ cm using the same parameters as in Fig. 4. Clearly, the shapes of three input fields have changed

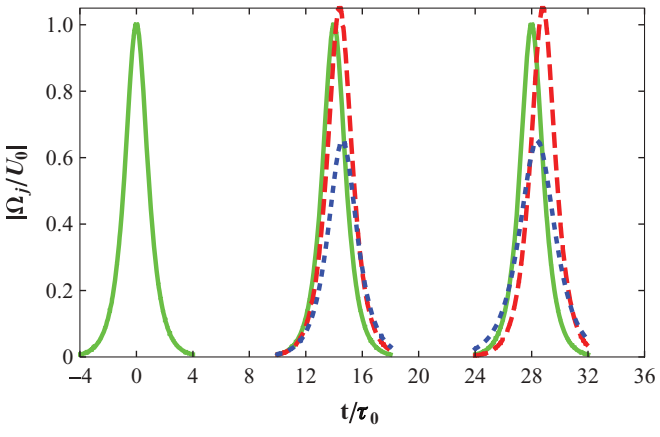

FIG. 5. (Color online) Comparison of analytical solutions of Eqs. (63)–(62) (dashed lines) and the full numerical solutions (solid lines) obtained by directly integrating Eqs. (1)–(11) without using any approximations. The dotted lines are numerical solutions without including nonlinear terms (i.e., without SPM and CPM terms). Each curve contains three indistinguishable traces, that is, $|\Omega_a/U_0|$, $|\Omega_b/U_0|$, and $|\Omega_c/U_0|$. The parameters (Δ_j, γ_{ij}, Ω_d, U_0, τ, and $\kappa_{41,42,43}$) are the same as in Fig. 4.

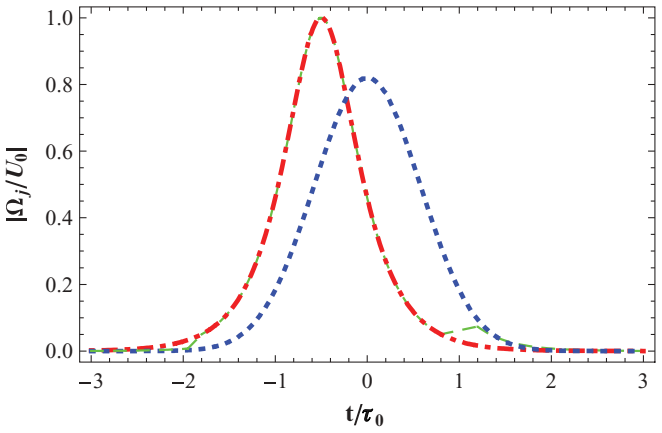

FIG. 6. (Color online) $|\Omega_a/U_0|$, $|\Omega_b/U_0|$, and $|\Omega_c/U_0|$ (dashed line) at $z = 0.8$ cm obtained by numerically integrating Eqs. (1)–(11) using three matched Gaussian input pulses. The central peak has a hyperbolic secant shape (dash-dotted line) and has an apparent advancement relative to that of the signal pulses propagating through a vacuum (dotted line). Each curve contains three indistinguishable traces.

significantly because the input signal fields are not a soliton. As a result of the nonlinear effects, the input pulses are narrowed, and they arrive at a balance by the dispersions of the system. One can find that the central peaks of the signal pulses can be fitted very well by a hyperbolic secant function (shown by the dash-dotted line) and have an apparent advancement relative to that of the signal fields propagating through a vacuum (shown by the dotted line), indicating that the shape preservation is well maintained at even $z = 0.8$ cm.

Before concluding, we need to explain why three coupled solitons with ultraslow group velocities cannot be formed under the resonant conditions ($\Delta_1 = \Delta_2 = 0$). The ultraslow propagation requires weak driving conditions, which leads to very narrow transparency windows [18]. Deviations from these conditions result in significant prove field attenuation and distortion. From Eqs. (44)–(52), however, it is clear that the nonlinear coefficient U_{ij} is closed and purely imaginary with small values of Δ_3 and Δ_4 (i.e., Δ_3, $\Delta_4 \sim 0$). This is contradictory to the requirement that U_{ij} be predominately real to obtain the soliton solutions of nonlinear Schrödinger equations (14)–(16).

However, although the present study focuses only on lifetime broadened atomic systems, the effects of Doppler broadening due to the different thermal velocity v can be included by first rewriting the corresponding velocity-dependent detunings, that is, $\Delta_1 = \omega_a - \epsilon_4 \Rightarrow \Delta_1 - k_{az}v_z$, $\Delta_2 = \omega_a + \omega_d - \epsilon_5 \Rightarrow \Delta_2 - (k_{dz}v_z \pm k_{bz}v_z)$, $\Delta_3 = \omega_a - \omega_b - \epsilon_2 \Rightarrow \Delta_3 - (k_{dz}v_z \pm k_{cz}v_z)$, and $\Delta_4 = \omega_a - \omega_c - \epsilon_3 \Rightarrow \Delta_2 - (k_{dz}v_z \pm k_{bz}v_z + k_{cz}v_z)$. The v_z-dependent quantities obtained are then averaged over a given velocity distribution $f(v_z)$ [29]. The qualitative analysis can be done by replacing the velocity v_z by $v \propto \sqrt{\langle v_z^2 \rangle}$ and $\langle v_z^2 \rangle = \int v_z^2 f(v_z) dv_z$. Obviously, a proper choice of the propagation directions of the waves can (sometimes greatly) decrease the effects of Doppler broadening.

In summary, we have proposed a scheme to produce three-component USOSs in a five-level tripod atomic system.

In the presence of a control field, linear as well as nonlinear dispersions are dramatically enhanced while simultaneously the absorptions of three pulsed probe fields are almost suppressed under appropriate conditions in the medium. In order to obtain the corresponding nonlinear evolution equations (i.e., three-coupled NLSE), we have employed the perturbation approach to the density matrix equations. We have also shown that detrimental distortions of probe fields due to strong dispersion effects under weak driving conditions can be well balanced by SPM and CPM effects, resulting in the three coupled optical solitons of different frequencies with nearly matched group velocity and amplitude. We also demonstrated that there exist parameter regimes in which the three coupled temporal optical solitons can be produced in a small distance ($L \sim 0.63$ cm) and propagate through the present system with ultraslow group velocities ($V_{gj} \sim 10^{-3}c$), which is in startling contrast to the soliton in optical fibers where the propagating velocity of the soliton is close to a vacuum light velocity and requires a substantial propagation distance. In addition, we stress that the three coupled USOSs predicted here can be established under very weak excitations, with the $\frac{1}{2}$ Rabi frequency of the driving field less than 100 MHz. Finally, we point out that the method described here is readily applicable to other excitation schemes with different atom configurations and also that our scheme may provide the possibility of promising applications for the design of new types of all-optical switches and logic gates in nonlinear optics and quantum information processing.

ACKNOWLEDGMENTS

The research was supported in part by the National Natural Science Foundation of China under Grant Nos. 10704017 and 10874050 and by the National Fundamental Research Program of China under Grant Nos. 2005CB724508 and 2007CB936300.

APPENDIX

The explicit expressions of terms K_a, K'_a, and K''_a in Eq. (21) are given by

$$K_a = \frac{\kappa_{41} d_{12}}{3(|\Omega_d|^2 - d_{11}d_{12})}, \tag{A1}$$

$$K'_a = \frac{1}{c} + \frac{\kappa_{41}\left(d_{12}^2 + d_{11}d_{12}\right)}{3(|\Omega_d|^2 - d_{11}d_{12})^2} + \frac{\kappa_{41}}{3(|\Omega_d|^2 - d_{11}d_{12})}, \tag{A2}$$

$$K''_a = \frac{\kappa_{41}\left(d_{11}^2 d_{12} + 2d_{11}d_{12}^2 + d_{12}^3\right)}{3(|\Omega_d|^2 - d_{11}d_{12})^3} + \frac{\kappa_{41}(d_{11} + 2d_{12})}{3(|\Omega_d|^2 - d_{11}d_{12})^2}; \tag{A3}$$

K_b, K'_b, and K''_b in Eq. (22) are given by

$$K_b = \frac{\kappa_{42} d_{22}}{3(|\Omega_d|^2 - d_{21}d_{22})}, \tag{A4}$$

$$K'_b = \frac{1}{c} + \frac{\kappa_{42}\left(1 + d_{22}^2 + d_{21}d_{22}\right)}{3(|\Omega_d|^2 - d_{21}d_{22})^2} + \frac{\kappa_{42}}{3(|\Omega_d|^2 - d_{21}d_{22})^2}, \tag{A5}$$

$$K''_b = \frac{\kappa_{42}\left(d_{21}^2 d_{22} + 2d_{21}d_{22}^2 + d_{22}^3\right)}{3(|\Omega_d|^2 - d_{21}d_{22})^3} + \frac{\kappa_{42}(d_{21} + 2d_{22})}{3(|\Omega_d|^2 - d_{21}d_{22})^2}; \tag{A6}$$

and K_c, K'_c, and K''_c in Eq. (23) are given by

$$K_b = \frac{\kappa_{43} d_{32}}{3(|\Omega_d|^2 - d_{31}d_{32})}, \tag{A7}$$

$$K'_b = \frac{1}{c} + \frac{\kappa_{43}\left(1 + d_{32}^2 + d_{31}d_{32}\right)}{3(|\Omega_d|^2 - d_{31}d_{32})^2} + \frac{\kappa_{43}}{3(|\Omega_d|^2 - d_{31}d_{32})^2}, \tag{A8}$$

$$K''_b = \frac{\kappa_{43}\left(d_{31}^2 d_{32} + 2d_{31}d_{32}^2 + d_{32}^3\right)}{3(|\Omega_d|^2 - d_{31}d_{32})^3} + \frac{\kappa_{43}(d_{31} + 2d_{32})}{3(|\Omega_d|^2 - d_{31}d_{32})^2}. \tag{A9}$$

[1] C. R. Menyuk, Opt. Lett. **12**, 614 (1987).
[2] D. N. Christodoulides and R. I. Joseph, Opt. Lett. **13**, 53 (1988).
[3] M. V. Tratnik and J. E. Sipe, Phys. Rev. A **38**, 2011 (1988).
[4] M. N. Islam, C. D. Poole, and J. P. Gordon, Opt. Lett. **14**, 1011 (1989).
[5] Y. Barad and Y. Silberberg, Phys. Rev. Lett. **78**, 3290 (1997).
[6] S. T. Cundiff, B. C. Collings, N. N. Akhmediev, J. M. Soto-Crespo, K. Bergman, and W. H. Knox, Phys. Rev. Lett. **82**, 3988 (1999).
[7] A. E. Korolev, V. N. Nazarov, D. A. Nolan, and C. M. Truesdale, Opt. Lett. **30**, 132 (2005).
[8] D. Rand, I. Glesk, C.-S. Bres, D. A. Nolan, X. Chen, J. Koh, J. W. Fleischer, K. Steiglitz, and P. R. Prucnal, Phys. Rev. Lett. **98**, 053902 (2007).
[9] M. Segev, G. C. Valley, B. Crosignani, P. DiPorto, and A. Yariv, Phys. Rev. Lett. **73**, 3211 (1994).
[10] Z. Chen, M. Segev, T. H. Coskun, and D. N. Christodoulides, Opt. Lett. **21**, 1436 (1996).
[11] J. U. Kang, G. I. Stegeman, J. S. Aitchison, and N. Akhmediev, Phys. Rev. Lett. **76**, 3699 (1996).
[12] C. Anastassiou, J. W. Fleischer, T. Carmon, M. Segev, and K. Steiglitz, Opt. Lett. **26**, 1498 (2001).
[13] M. Delquè, T. Sylvestre, H. Maillotte, C. Cambournac, P. Kockaert, and M. Haelterman, Opt. Lett. **30**, 3383 (2005).
[14] M. N. Islam, *Ultrafast Fiber Switching Devices and Systems* (Cambridge University Press, Cambridge, 1992).
[15] Y. S. Kivshar and G. P. Agrawal, *Optical Solitons: From Fibers to Photonic Crystals* (Academic Press, San Diego, 2003).
[16] S. V. Manakov, Sov. Phys. JETP **38**, 248 (1974).
[17] K. Steiglitz, Phys. Rev. E **63**, 016608 (2000).
[18] M. Fleischhauer, A. Imamoglu, and J. P. Marangos, Rev. Mod. Phys. **77**, 633 (2005).
[19] H. Schmidt and A. Imamoglu, Opt. Lett. **21**, 1936 (1996).
[20] S. E. Harris and L. V. Hau, Phys. Rev. Lett. **82**, 4611 (1999).
[21] M. D. Lukin and A. Imamoglu, Phys. Rev. Lett. **84**, 1419 (2000).
[22] D. F. Phillips, A. Fleischhauer, A. Mair, R. L. Walsworth, and M. D. Lukin, Phys. Rev. Lett. **86**, 783 (2001).

[23] D. Petrosyan and G. Kurizki, Phys. Rev. A **65**, 033833 (2002).
[24] Y. Wu and X. Yang, Phys. Rev. A **71**, 053806 (2005).
[25] Y. Wu and X. Yang, Phys. Rev. A **70**, 053818 (2004).
[26] D. Petrosyan and Y. P. Malakyan, Phys. Rev. A **70**, 023822 (2004).
[27] S. Rebić, D. Vitali, C. Ottaviani, P. Tombesi, M. Artoni, F. Cataliotti, and R. Corbalán, Phys. Rev. A **70**, 032317 (2004).
[28] L. V. Hau *et al.*, Nature (London) **397**, 594 (1999).
[29] M. M. Kash, V. A. Sautenkov, A. S. Zibrov, L. Hollberg, G. R. Welch, M. D. Lukin, Y. Rostovtsev, E. S. Fry, and M. O. Scully, Phys. Rev. Lett. **82**, 5229 (1999).
[30] J. E. Heebner, R. W. Boyd, and Q. H. Park, Phys. Rev. E **65**, 036619 (2002).
[31] Y. Wu and L. Deng, Phys. Rev. Lett. **93**, 143904 (2004).
[32] Y. Wu and L. Deng, Opt. Lett. **29**, 2064 (2004).
[33] G. Huang, L. Deng, and M. G. Payne, Phys. Rev. E **72**, 016617 (2005).
[34] L. Deng, M. G. Payne, G. Huang, and E. W. Hagley, Phys. Rev. E **72**, 055601(R) (2005).
[35] X.-T. Xie, W.-B. Li, and X. Yang, J. Opt. Soc. Am. B **23**, 1609 (2006).
[36] C. Hang, G. Huang, and L. Deng, Phys. Rev. E **73**, 036607 (2006).
[37] W.-X. Yang, J.-M. Hou, and R.-K. Lee, Phys. Rev. A **77**, 033838 (2008).
[38] W.-X. Yang and R.-K. Lee, Europhys. Lett. **83**, 14002 (2008).
[39] W.-X. Yang, J.-M. Hou, Y. Y. Lin, and R.-K. Lee, Phys. Rev. A **79**, 033825 (2009).
[40] A. E. Kaplan, P. L. Shkolnikov, and B. A. Akanaev, Opt. Lett. **19**, 445 (1994).
[41] A. E. Kaplan, Phys. Rev. Lett. **73**, 1243 (1994).
[42] Y. Wu, Phys. Rev. A **71**, 053820 (2005).
[43] G. Huang, K. J. Jiang, M. G. Payne, and L. Deng, Phys. Rev. E **73**, 056606 (2006).
[44] H. Michinel, M. J. Paz-Alonso, and V. M. Perez-Garcia, Phys. Rev. Lett. **96**, 023903 (2006).
[45] I. Friedler, G. Kurizki, O. Cohen, and M. Segev, Opt. Lett. **30**, 3374 (2005).
[46] T. Hong, Phys. Rev. Lett. **90**, 183901 (2003).
[47] C. Hang and G. Huang, Phys. Rev. A **77**, 033830 (2008).
[48] L. G. Si, W. X. Yang, J. B. Liu, J. Li, and X. Yang, Opt. Express **17**, 7771 (2009).
[49] L. G. Si, W. X. Yang, and X. Yang, J. Opt. Soc. Am. B **26**, 478 (2009).
[50] Y. Wu, Phys. Rev. A **71**, 053820 (2005).
[51] D. V. Skryabin, F. Biancalana, D. M. Bird, and F. Benabid, Phys. Rev. Lett. **93**, 143907 (2004).
[52] F. T. Hioe, Phys. Rev. Lett. **82**, 1152 (1999).
[53] K. Nakkeeran, Phys. Rev. E **62**, 1313 (2000).
[54] M. Yan, E. G. Rickey, and Y. Zhu, Phys. Rev. A **64**, 043807 (2001).
[55] V. M. Petnikova, V. V. Shuvalov, and V. A. Vysloukh, Phys. Rev. E **60**, 1009 (1999).
[56] A. A. Sukhorukov and N. N. Akhmediev, Phys. Rev. Lett. **83**, 4736 (1999).